

# Measurement of branching fractions for $B \rightarrow J/\psi\eta K$ decays and search for a narrow resonance in the $J/\psi\eta$ final state

T. Iwashita,<sup>40</sup> K. Miyabayashi,<sup>40</sup> V. Bhardwaj,<sup>40</sup> I. Adachi,<sup>14</sup> H. Aihara,<sup>62</sup> D. M. Asner,<sup>49</sup> T. Aushev,<sup>24</sup> A. M. Bakich,<sup>56</sup> A. Bala,<sup>50</sup> B. Bhuyan,<sup>17</sup> G. Bonvicini,<sup>68</sup> A. Bozek,<sup>44</sup> M. Bračko,<sup>34,25</sup> T. E. Browder,<sup>13</sup> M.-C. Chang,<sup>8</sup> A. Chen,<sup>41</sup> B. G. Cheon,<sup>12</sup> K. Chilikin,<sup>24</sup> R. Chistov,<sup>24</sup> K. Cho,<sup>29</sup> V. Chobanova,<sup>35</sup> S.-K. Choi,<sup>11</sup> Y. Choi,<sup>55</sup> D. Cinabro,<sup>68</sup> J. Dalseno,<sup>35,58</sup> M. Danilov,<sup>24,37</sup> Z. Doležal,<sup>5</sup> Z. Drásal,<sup>5</sup> D. Dutta,<sup>17</sup> S. Eidelman,<sup>4</sup> S. Esen,<sup>6</sup> H. Farhat,<sup>68</sup> J. E. Fast,<sup>49</sup> M. Feindt,<sup>27</sup> T. Ferber,<sup>7</sup> A. Frey,<sup>10</sup> V. Gaur,<sup>57</sup> N. Gabyshev,<sup>4</sup> S. Ganguly,<sup>68</sup> R. Gillard,<sup>68</sup> Y. M. Goh,<sup>12</sup> B. Golob,<sup>33,25</sup> J. Haba,<sup>14</sup> T. Hara,<sup>14</sup> K. Hayasaka,<sup>39</sup> H. Hayashii,<sup>40</sup> T. Higuchi,<sup>28</sup> Y. Horii,<sup>39</sup> Y. Hoshi,<sup>60</sup> W.-S. Hou,<sup>43</sup> H. J. Hyun,<sup>31</sup> T. Iijima,<sup>39,38</sup> A. Ishikawa,<sup>61</sup> R. Itoh,<sup>14</sup> Y. Iwasaki,<sup>14</sup> I. Jaegle,<sup>13</sup> T. Julius,<sup>36</sup> D. H. Kah,<sup>31</sup> J. H. Kang,<sup>70</sup> E. Kato,<sup>61</sup> T. Kawasaki,<sup>46</sup> H. Kichimi,<sup>14</sup> C. Kiesling,<sup>35</sup> D. Y. Kim,<sup>54</sup> H. J. Kim,<sup>31</sup> H. O. Kim,<sup>31</sup> J. B. Kim,<sup>30</sup> J. H. Kim,<sup>29</sup> M. J. Kim,<sup>31</sup> Y. J. Kim,<sup>29</sup> K. Kinoshita,<sup>6</sup> J. Klucar,<sup>25</sup> B. R. Ko,<sup>30</sup> P. Kodyš,<sup>5</sup> S. Korpar,<sup>34,25</sup> P. Krizán,<sup>33,25</sup> P. Krokovny,<sup>4</sup> T. Kuhr,<sup>27</sup> T. Kumita,<sup>64</sup> A. Kuzmin,<sup>4</sup> Y.-J. Kwon,<sup>70</sup> J. S. Lange,<sup>9</sup> S.-H. Lee,<sup>30</sup> Y. Li,<sup>67</sup> J. Libby,<sup>18</sup> C. Liu,<sup>52</sup> Y. Liu,<sup>6</sup> P. Lukin,<sup>4</sup> D. Matvienko,<sup>4</sup> H. Miyata,<sup>46</sup> R. Mizuk,<sup>24,37</sup> A. Moll,<sup>35,58</sup> T. Mori,<sup>38</sup> Y. Nagasaka,<sup>15</sup> E. Nakano,<sup>48</sup> M. Nakao,<sup>14</sup> H. Nakazawa,<sup>41</sup> Z. Natkaniec,<sup>44</sup> M. Nayak,<sup>18</sup> C. Ng,<sup>62</sup> N. K. Nisar,<sup>57</sup> S. Nishida,<sup>14</sup> O. Nitoh,<sup>65</sup> S. Ogawa,<sup>59</sup> S. Okuno,<sup>26</sup> G. Pakhlova,<sup>24</sup> E. Panzenböck,<sup>10,40</sup> H. Park,<sup>31</sup> H. K. Park,<sup>31</sup> T. K. Pedlar,<sup>71</sup> R. Pestotnik,<sup>25</sup> M. Petrič,<sup>25</sup> L. E. Piilonen,<sup>67</sup> M. Ritter,<sup>35</sup> M. Röhrken,<sup>27</sup> A. Rostomyan,<sup>7</sup> S. Ryu,<sup>53</sup> H. Sahoo,<sup>13</sup> T. Saito,<sup>61</sup> K. Sakai,<sup>14</sup> Y. Sakai,<sup>14</sup> S. Sandilya,<sup>57</sup> D. Santel,<sup>6</sup> L. Santelj,<sup>25</sup> T. Sanuki,<sup>61</sup> V. Savinov,<sup>51</sup> O. Schneider,<sup>32</sup> G. Schnell,<sup>1,16</sup> C. Schwanda,<sup>21</sup> D. Semmler,<sup>9</sup> K. Senyo,<sup>69</sup> O. Seon,<sup>38</sup> M. E. Sevier,<sup>36</sup> M. Shapkin,<sup>22</sup> C. P. Shen,<sup>2</sup> T.-A. Shibata,<sup>63</sup> J.-G. Shiu,<sup>43</sup> B. Shwartz,<sup>4</sup> A. Sibidanov,<sup>56</sup> F. Simon,<sup>35,58</sup> Y.-S. Sohn,<sup>70</sup> A. Sokolov,<sup>22</sup> E. Solovieva,<sup>24</sup> S. Stanič,<sup>47</sup> M. Starič,<sup>25</sup> M. Steder,<sup>7</sup> T. Sumiyoshi,<sup>64</sup> U. Tamponi,<sup>23,66</sup> K. Tanida,<sup>53</sup> G. Tatishvili,<sup>49</sup> Y. Teramoto,<sup>48</sup> K. Trabelsi,<sup>14</sup> T. Tsuboyama,<sup>14</sup> M. Uchida,<sup>63</sup> S. Uehara,<sup>14</sup> Y. Unno,<sup>12</sup> S. Uno,<sup>14</sup> P. Urquijo,<sup>3</sup> P. Vanhosefer,<sup>35</sup> G. Varner,<sup>13</sup> K. E. Varvell,<sup>56</sup> V. Vorobyev,<sup>4</sup> A. Vossen,<sup>19</sup> M. N. Wagner,<sup>9</sup> C. H. Wang,<sup>42</sup> M.-Z. Wang,<sup>43</sup> P. Wang,<sup>20</sup> X. L. Wang,<sup>67</sup> M. Watanabe,<sup>46</sup> Y. Watanabe,<sup>26</sup> K. M. Williams,<sup>67</sup> E. Won,<sup>30</sup> B. D. Yabsley,<sup>56</sup> Y. Yamashita,<sup>45</sup> S. Yashchenko,<sup>7</sup> Y. Yook,<sup>70</sup> C. Z. Yuan,<sup>20</sup> Z. P. Zhang,<sup>52</sup> V. Zhilich,<sup>4</sup> and A. Zupanc<sup>27</sup>

(The Belle Collaboration)

<sup>1</sup>University of the Basque Country UPV/EHU, 48080 Bilbao

<sup>2</sup>Beihang University, Beijing 100191

<sup>3</sup>University of Bonn, 53115 Bonn

<sup>4</sup>Budker Institute of Nuclear Physics SB RAS and Novosibirsk State University, Novosibirsk 630090

<sup>5</sup>Faculty of Mathematics and Physics, Charles University, 121 16 Prague

<sup>6</sup>University of Cincinnati, Cincinnati, Ohio 45221

<sup>7</sup>Deutsches Elektronen-Synchrotron, 22607 Hamburg

<sup>8</sup>Department of Physics, Fu Jen Catholic University, Taipei 24205

<sup>9</sup>Justus-Liebig-Universität Gießen, 35392 Gießen

<sup>10</sup>II. Physikalisches Institut, Georg-August-Universität Göttingen, 37073 Göttingen

<sup>11</sup>Gyeongsang National University, Chinju 660-701

<sup>12</sup>Hanyang University, Seoul 133-791

<sup>13</sup>University of Hawaii, Honolulu, Hawaii 96822

<sup>14</sup>High Energy Accelerator Research Organization (KEK), Tsukuba 305-0801

<sup>15</sup>Hiroshima Institute of Technology, Hiroshima 731-5193

<sup>16</sup>Ikerbasque, 48011 Bilbao

<sup>17</sup>Indian Institute of Technology Guwahati, Assam 781039

<sup>18</sup>Indian Institute of Technology Madras, Chennai 600036

<sup>19</sup>Indiana University, Bloomington, Indiana 47408

<sup>20</sup>Institute of High Energy Physics, Chinese Academy of Sciences, Beijing 100049

<sup>21</sup>Institute of High Energy Physics, Vienna 1050

<sup>22</sup>Institute for High Energy Physics, Protvino 142281

<sup>23</sup>INFN - Sezione di Torino, 10125 Torino

<sup>24</sup>Institute for Theoretical and Experimental Physics, Moscow 117218

<sup>25</sup>J. Stefan Institute, 1000 Ljubljana

<sup>26</sup>Kanagawa University, Yokohama 221-8686

<sup>27</sup>Institut für Experimentelle Kernphysik, Karlsruher Institut für Technologie, 76131 Karlsruhe

<sup>28</sup>Kavli Institute for the Physics and Mathematics of the Universe (WPI), University of Tokyo, Kashiwa 277-8583

<sup>29</sup>Korea Institute of Science and Technology Information, Daejeon 305-806

<sup>30</sup>Korea University, Seoul 136-713

- <sup>31</sup>Kyungpook National University, Daegu 702-701  
<sup>32</sup>École Polytechnique Fédérale de Lausanne (EPFL), Lausanne 1015  
<sup>33</sup>Faculty of Mathematics and Physics, University of Ljubljana, 1000 Ljubljana  
<sup>34</sup>University of Maribor, 2000 Maribor  
<sup>35</sup>Max-Planck-Institut für Physik, 80805 München  
<sup>36</sup>School of Physics, University of Melbourne, Victoria 3010  
<sup>37</sup>Moscow Physical Engineering Institute, Moscow 115409  
<sup>38</sup>Graduate School of Science, Nagoya University, Nagoya 464-8602  
<sup>39</sup>Kobayashi-Maskawa Institute, Nagoya University, Nagoya 464-8602  
<sup>40</sup>Nara Women's University, Nara 630-8506  
<sup>41</sup>National Central University, Chung-li 32054  
<sup>42</sup>National United University, Miao Li 36003  
<sup>43</sup>Department of Physics, National Taiwan University, Taipei 10617  
<sup>44</sup>H. Niewodniczanski Institute of Nuclear Physics, Krakow 31-342  
<sup>45</sup>Nippon Dental University, Niigata 951-8580  
<sup>46</sup>Niigata University, Niigata 950-2181  
<sup>47</sup>University of Nova Gorica, 5000 Nova Gorica  
<sup>48</sup>Osaka City University, Osaka 558-8585  
<sup>49</sup>Pacific Northwest National Laboratory, Richland, Washington 99352  
<sup>50</sup>Panjab University, Chandigarh 160014  
<sup>51</sup>University of Pittsburgh, Pittsburgh, Pennsylvania 15260  
<sup>52</sup>University of Science and Technology of China, Hefei 230026  
<sup>53</sup>Seoul National University, Seoul 151-742  
<sup>54</sup>Soongsil University, Seoul 156-743  
<sup>55</sup>Sungkyunkwan University, Suwon 440-746  
<sup>56</sup>School of Physics, University of Sydney, NSW 2006  
<sup>57</sup>Tata Institute of Fundamental Research, Mumbai 400005  
<sup>58</sup>Excellence Cluster Universe, Technische Universität München, 85748 Garching  
<sup>59</sup>Toho University, Funabashi 274-8510  
<sup>60</sup>Tohoku Gakuin University, Tagajo 985-8537  
<sup>61</sup>Tohoku University, Sendai 980-8578  
<sup>62</sup>Department of Physics, University of Tokyo, Tokyo 113-0033  
<sup>63</sup>Tokyo Institute of Technology, Tokyo 152-8550  
<sup>64</sup>Tokyo Metropolitan University, Tokyo 192-0397  
<sup>65</sup>Tokyo University of Agriculture and Technology, Tokyo 184-8588  
<sup>66</sup>University of Torino, 10124 Torino  
<sup>67</sup>CNP, Virginia Polytechnic Institute and State University, Blacksburg, Virginia 24061  
<sup>68</sup>Wayne State University, Detroit, Michigan 48202  
<sup>69</sup>Yamagata University, Yamagata 990-8560  
<sup>70</sup>Yonsei University, Seoul 120-749  
<sup>71</sup>Luther College, Decorah, Iowa 52101

We report an observation of the  $B^\pm \rightarrow J/\psi\eta K^\pm$  and  $B^0 \rightarrow J/\psi\eta K_S^0$  decays using  $772 \times 10^6$   $B\bar{B}$  pairs collected at the  $\Upsilon(4S)$  resonance with the Belle detector at the KEKB asymmetric-energy  $e^+e^-$  collider. We obtain the branching fractions  $\mathcal{B}(B^\pm \rightarrow J/\psi\eta K^\pm) = (1.27 \pm 0.11(\text{stat.}) \pm 0.11(\text{syst.})) \times 10^{-4}$  and  $\mathcal{B}(B^0 \rightarrow J/\psi\eta K_S^0) = (5.22 \pm 0.78(\text{stat.}) \pm 0.49(\text{syst.})) \times 10^{-5}$ . We search for a new narrow charmonium(-like) state  $X$  in the  $J/\psi\eta$  mass spectrum and find no significant excess. We set upper limits on the product of branching fractions,  $\mathcal{B}(B^\pm \rightarrow XK^\pm)\mathcal{B}(X \rightarrow J/\psi\eta)$ , at 3872 MeV/ $c^2$  where a  $C$ -odd partner of  $X(3872)$  may exist, at  $\psi(4040)$  and  $\psi(4160)$  assuming their known mass and width, and over a range from 3.8 to 4.8 GeV/ $c^2$ . The obtained upper limits at 90% confidence level for  $X^{C\text{-odd}}(3872)$ ,  $\psi(4040)$  and  $\psi(4160)$  are  $3.8 \times 10^{-6}$ ,  $15.5 \times 10^{-6}$  and  $7.4 \times 10^{-6}$ , respectively.

PACS numbers: 13.25.-k, 14.40.-n

The discovery of a narrow charmonium-like resonance,  $X(3872)$ , in the  $J/\psi\pi^+\pi^-$  final state by the Belle collaboration in 2003 [1] opened a new era in the spectroscopy of charmonium and charmonium-like exotic states [2]. In addition to  $J/\psi\pi^+\pi^-$ ,  $X(3872)$  decays are also seen in the  $D^0\bar{D}^{*0}$  [3],  $J/\psi\pi^+\pi^-\pi^0$  [4] and  $J/\psi\gamma$  [5, 6] final states. Observation of the  $X(3872) \rightarrow J/\psi\gamma$  mode confirms that its  $C$ -parity is even. The studies of angular distributions of the decay products in the  $X(3872) \rightarrow J/\psi\pi^+\pi^-$  mode by CDF [7] and Belle [8] as well as the  $3\pi$  invariant mass spectrum in  $J/\psi\pi^+\pi^-\pi^0$  mode by BaBar [4] restrict  $J^{PC}$  to be either  $1^{++}$  and  $2^{-+}$  but do not allow a definitive determination. A full five-dimensional amplitude analysis of the angles among the decay products

in  $B^+ \rightarrow X(3872)K^+$ ,  $X(3872) \rightarrow J/\psi\pi^+\pi^-$  recently performed by the LHCb collaboration has unambiguously assigned  $J^{PC} = 1^{++}$  to the  $X(3872)$  [9].

The very small width ( $\Gamma < 1.2$  MeV) [8] of the  $X(3872)$  and its mass ( $M = 3871.7 \pm 0.2$  MeV/ $c^2$ ) close to the  $D^0\bar{D}^{*0}$  threshold [10] make its interpretation as a  $D^0\bar{D}^{*0}$  molecule [11] quite plausible. However, other models such as tetraquark [12], hybrid ( $c\bar{c}g$ ) [13] and the admixture of molecular and charmonium states [14] are not excluded. In both the molecule and tetraquark pictures [15, 16], a  $C$ -odd partner ( $X^{C\text{-odd}}$ ) or a charged partner ( $X^\pm$ ) of  $X(3872)$  can exist. So far, searches for the charged partner  $X^\pm \rightarrow J/\psi\pi^\pm\pi^0$  have given negative results [8, 17]. This might be only because the  $X^\pm$  is too broad, given the current statistics; it leaves open the possibility of a moderately narrow  $C$ -odd partner, as postulated by the tetraquark model [15]. Recently, the Belle collaboration has searched for the  $X^{C\text{-odd}} \rightarrow \chi_{c1}\gamma$  transition in  $B \rightarrow \chi_{c1}\gamma K$  decays and reported evidence for a narrow resonance at 3823 MeV/ $c^2$  [18]. This resonance is presumably the  $1^3D_2$   $c\bar{c}$  ( $\psi_2$ ) rather than the  $X^{C\text{-odd}}$ , since its mass, decay width and the discovery decay mode are consistent with theoretical prediction for this charmonium state [19–21].

Alternatively, the  $X^{C\text{-odd}}$  might appear in the  $J/\psi\eta$  final state. The photon energy in  $\eta \rightarrow \gamma\gamma$  is well above the energy threshold to be detected in  $B$ -factory experiments even in the case where the resonance is just above the  $J/\psi\eta$  mass threshold. Therefore, the  $J/\psi\eta$  system in the three-body  $B \rightarrow J/\psi\eta K$  decay is a suitable final state to search for a missing  $C$ -odd partner of the  $X(3872)$  as well as any yet-unseen charmonium(-like) resonances. The  $J/\psi\eta$  final state is also sensitive to the  $\psi(4040)$  and  $\psi(4160)$  resonances, whose decays into  $J/\psi\eta$  were recently reported by BESIII in  $e^+e^-$  annihilation [22] and Belle in the initial state radiation process [23]. Since the total width and partial width to  $e^+e^-$  are known for these charmonia [10], this observation implies  $\psi(4040)$  and  $\psi(4160)$  have branching fractions of a few percent to  $J/\psi\eta$ . If the branching fractions for  $B^\pm \rightarrow \psi(4040)K^\pm$  or  $\psi(4160)K^\pm$  are as high as  $\sim 10^{-3}$ , these decay channels are accessible with Belle's data set.

The branching fraction for  $B \rightarrow J/\psi\eta K$  decay may also shed light on the inclusive spectrum of  $B \rightarrow J/\psi X$ , which is fairly well described by non-relativistic QCD calculations [24] except for an excess in the low momentum region [25, 26]. There have been several models proposed to explain this excess, such as  $B \rightarrow J/\psi K_g$  (where  $K_g$  is a hybrid meson with  $\bar{s}qg$  constituents) [27], or a still-undiscovered charmonium(-like) state that decays into  $J/\psi$  [28]. Such exotic or new states can be constrained by measurements of multibody  $B$  decay modes into  $J/\psi$ , such as  $B \rightarrow J/\psi\eta K$ , because they populate the region of the above-mentioned excess.

A previous study by the BaBar collaboration [29] reported an observation of  $B^\pm \rightarrow J/\psi\eta K^\pm$  and evidence for  $B^0 \rightarrow J/\psi\eta K_S^0$  [30] using  $90 \times 10^6$   $B\bar{B}$  pairs ( $N_{B\bar{B}}$ ), but no signal of a narrow resonance was found in the  $J/\psi\eta$  spectrum. In this paper, we present a study of  $B \rightarrow J/\psi\eta K$  decays based on a data sample of  $772 \times 10^6$   $B\bar{B}$  events collected with the Belle detector at the KEKB asymmetric-energy  $e^+e^-$  collider [31] at the  $\Upsilon(4S)$  resonance.

The Belle detector is a large solid-angle magnetic spectrometer that consists of a silicon vertex detector (SVD), a 50-layer central drift chamber (CDC), an array of aerogel threshold Cherenkov counters (ACC), a barrel-like arrangement of time-of-flight scintillation counters (TOF), and an electromagnetic calorimeter (ECL) comprised of CsI(Tl) crystals located inside a superconducting solenoid coil that provides a 1.5 T magnetic field. An iron flux return located outside of the coil is instrumented to detect  $K_L^0$  mesons and to identify muons (KLM). The detector is described in detail elsewhere [32]. Two inner detector configurations were used. A 2.0 cm radius beampipe and a three-layer silicon vertex detector were used to collect the first sample of  $152 \times 10^6$   $B\bar{B}$  pairs, while a 1.5 cm radius beampipe, a four-layer silicon detector and a small-cell inner drift chamber were used to record the remaining  $620 \times 10^6$   $B\bar{B}$  pairs [33].

Charged tracks coming from  $B$  decays should originate from the interaction point (IP). The closest approach with respect to the IP is required to be within 5.0 cm along the beam direction ( $z$ -axis) and within 2.0 cm in the transverse plane. Photons are reconstructed as ECL clusters without an associated charged track that have transverse shower shape variables consistent with an electromagnetic cascade hypothesis. For  $\eta$  reconstruction, the daughter photon has an energy greater than 100 MeV in the laboratory frame.

The  $J/\psi$  meson is reconstructed in its decay to  $\ell^+\ell^-$  ( $\ell = e$  or  $\mu$ ). From the selected charged tracks,  $e^\pm$  candidates are identified by combining specific-ionization ( $dE/dx$ ) information from the CDC,  $E/p$  (where  $E$  is the shower energy detected in the ECL and  $p$  is the momentum measured by the SVD and the CDC), and shower shape in the ECL. In addition, the ACC information and the position difference between the electron track candidate and the matching ECL cluster are used in the identification of electron candidates. In the  $J/\psi \rightarrow e^+e^-$  mode, in order to recover bremsstrahlung photons and final state radiation, the four-momenta of all photons within 50 mrad of each of the leptons are included in the invariant mass that is hereinafter denoted as  $M_{e^+e^-(\gamma)}$ . Identification of  $\mu$  candidates is based on the track penetration depth and hit pattern in the KLM system [34]. The reconstructed invariant mass of a  $J/\psi$  candidate must satisfy  $2.95$  GeV/ $c^2 < M_{e^+e^-(\gamma)} < 3.13$  GeV/ $c^2$  or  $3.04$  GeV/ $c^2 < M_{\mu^+\mu^-} < 3.13$  GeV/ $c^2$ . In order to improve the momentum resolution, a vertex-constrained fit followed by a mass-constrained fit is applied for the  $J/\psi$  candidates and convergence of both fits is required.

Pairs of photons are combined to form  $\eta$  candidates within the mass range  $510$  MeV/ $c^2 < M_{\gamma\gamma} < 575$  MeV/ $c^2$ . To

further reduce combinatorial background, the  $\eta \rightarrow \gamma\gamma$  candidates are required to have an energy balance parameter ( $|E_1 - E_2|/(E_1 + E_2)$ ) smaller than 0.8, where  $E_1$  ( $E_2$ ) is the energy of the first (second) photon in the laboratory frame. To suppress the background photons from  $\pi^0$  decays, we reject any photon forming a  $\pi^0$  candidate ( $117 \text{ MeV}/c^2 < M_{\gamma\gamma} < 153 \text{ MeV}/c^2$ ) with any other photon in the event. For the selected  $\eta$  candidates, a mass-constrained fit is performed to improve the momentum resolution.

Charged kaons are identified by combining information from the CDC, TOF and ACC systems. The kaon identification efficiency is about 90% while the probability of misidentifying a pion as a kaon is about 10% for the corresponding momentum range.  $K_S^0$  mesons are reconstructed by combining two oppositely charged tracks (both assumed to be pions) and requiring the invariant mass  $M_{\pi^+\pi^-}$  to be between 482 and 514  $\text{MeV}/c^2$ . The selected candidates are required to have a vertex displaced from the IP as described in Ref. [35].

A  $B \rightarrow J/\psi\eta K$  candidate is formed from the  $J/\psi$ ,  $\eta$  and kaon candidates and is identified by two kinematic variables defined in the  $\Upsilon(4S)$  rest frame (cms): the energy difference ( $\Delta E \equiv E_B^* - E_{\text{beam}}^*$ ) and the beam-energy constrained mass ( $M_{\text{bc}} \equiv \sqrt{(E_{\text{beam}}^*)^2 - (P_B^*)^2}$ ). Here,  $E_{\text{beam}}^*$  is the cms beam energy and  $E_B^*$  and  $P_B^*$  are the cms energy and momentum, respectively, of the reconstructed  $B$  candidate. Events having at least one  $B$  candidate satisfying  $M_{\text{bc}} > 5.27 \text{ GeV}/c^2$  and  $|\Delta E| < 0.2 \text{ GeV}$  are retained for further analysis.

Among the retained events, 29% have more than one  $B$  candidate. This is predominantly due to the wrong combination in forming the  $\eta$  candidate or, far less frequently, due to an incorrect  $J/\psi \rightarrow \ell^+\ell^-$  reconstruction; cases with an incorrect kaon candidate are negligible. Therefore, we select the  $B$  candidate having the smallest goodness of fit, defined as  $\chi^2 \equiv (M_{\ell^+\ell^-} - m_{J/\psi})^2/\sigma_{\ell^+\ell^-}^2 + (M_{\gamma\gamma} - m_\eta)^2/\sigma_{\gamma\gamma}^2$ , where  $M_{\ell^+\ell^-}$  denotes  $M_{e^+e^-(\gamma)}$  or  $M_{\mu^+\mu^-}$ ,  $\sigma_{\ell^+\ell^-}$  denotes the  $M_{\ell^+\ell^-}$  resolutions (11.1  $\text{MeV}/c^2$  for  $M_{e^+e^-(\gamma)}$  and 8.9  $\text{MeV}/c^2$  for  $M_{\mu^+\mu^-}$ ),  $M_{\gamma\gamma}$  is the photon pair mass, and  $\sigma_{\gamma\gamma}$  is the  $M_{\gamma\gamma}$  resolution (13.8  $\text{MeV}/c^2$ ). Here,  $m_{J/\psi}$  and  $m_\eta$  are the nominal meson masses [10].

To suppress continuum background, we reject events having a ratio  $R_2$  of the second to zeroth Fox-Wolfram moments [36] greater than 0.5. Among the backgrounds from  $B\bar{B}$  events, those that contain a real  $J/\psi \rightarrow \ell^+\ell^-$  decay dominate. A large sample of  $B \rightarrow J/\psi X$  Monte Carlo (MC) decays, corresponding to 100 times the data sample, is used to model this background component's  $M_{\text{bc}}$  and  $\Delta E$  distributions. When  $\psi'$  decays to the final states other than  $J/\psi\eta$ , the  $B \rightarrow \psi'K$  decay mode forms a significant portion of the background. We denote this contribution as the  $B \rightarrow \psi'(\not\rightarrow J/\psi\eta)K$  process. In order to reduce this background, we reject a  $J/\psi$  that, when combined with a  $\pi^+\pi^-$  pair, forms a  $\psi'$  candidate with a mass difference in the range  $0.58 \text{ GeV}/c^2 < M_{J/\psi\pi^+\pi^-} - m_{J/\psi} < 0.60 \text{ GeV}/c^2$ . The non- $J/\psi$  background is estimated using the  $M_{\ell^+\ell^-}$  sideband events in data and is found to be negligible.

The  $B$  decay signal extraction is carried out by performing an extended unbinned maximum likelihood (UML) fit to the  $\Delta E$  distribution. Figure. 1 shows the  $\Delta E$  distribution for the charged and neutral  $B$  decay candidates together with the fit results. Clear signal peaks are seen on smoothly distributing background for both cases. For these decays, a sum of two Gaussians is used to model the probability density function (PDF) for signal events. For the  $B^\pm \rightarrow J/\psi\eta K^\pm$  decay mode, the mean and width of the core Gaussian are floated and the remaining parameters are fixed to values obtained by fitting the signal MC distribution. Since we have smaller statistics for  $B^0 \rightarrow J/\psi\eta K_S^0$ , the parameters of the signal PDF is fixed to the values of data obtained by the  $B^\pm \rightarrow J/\psi\eta K^\pm$  sample. Since the  $B \rightarrow \psi'(\not\rightarrow J/\psi\eta)K$  and  $B \rightarrow \chi_{c1}K$  decay modes are expected to have different features compared to other backgrounds in the  $\Delta E$  distribution, these two processes are treated separately. We use a bifurcated Gaussian to describe these decay modes whose parameters are fixed from large MC simulation samples. Since the branching fractions for these decay modes are known [10], their yields are also fixed. To model the remaining featureless combinatorial background in the  $\Delta E$  projection, we use a second-order (first-order) Chebyshev polynomial for the  $B^\pm \rightarrow J/\psi\eta K^\pm$  ( $B^0 \rightarrow J/\psi\eta K_S^0$ ) decay mode. We obtain signal yields of  $428 \pm 37$  events and  $94 \pm 14$  events for the  $B^\pm \rightarrow J/\psi\eta K^\pm$  and  $B^0 \rightarrow J/\psi\eta K_S^0$  decay modes, respectively. The detection efficiency estimation for  $B^\pm \rightarrow J/\psi\eta K^\pm$  is described in more detail later. The three-body phase space distribution is assumed for  $B^0 \rightarrow J/\psi\eta K_S^0$ . Their branching fractions are  $(1.27 \pm 0.11 \pm 0.11) \times 10^{-4}$  and  $(5.22 \pm 0.78 \pm 0.49) \times 10^{-5}$ , where the first uncertainty is statistical and the second is systematic uncertainty; these uncertainties are described later in detail. We calculate the statistical significance,  $\sqrt{-2 \ln \mathcal{L}_0/\mathcal{L}_{\text{max}}}$ , where  $\mathcal{L}_{\text{max}}$  ( $\mathcal{L}_0$ ) denote the likelihood value when the signal yield is allowed to vary (is set to zero). The significance is found to be  $17\sigma$  ( $7\sigma$ ) for the  $B^\pm \rightarrow J/\psi\eta K^\pm$  ( $B^0 \rightarrow J/\psi\eta K_S^0$ ) decay mode. We observe the  $B^0 \rightarrow J/\psi\eta K_S^0$  decay mode for the first time with the significance more than  $5\sigma$ . Equal production of neutral and charged  $B$  meson pairs in the  $\Upsilon(4S)$  decay is assumed. We used the secondary branching fractions reported in Ref. [10]. The results of the fits are presented in Table I.

Since the  $B^\pm \rightarrow J/\psi\eta K^\pm$  signal is strong, we use the  $J/\psi\eta$  mass spectrum ( $M_{J/\psi\eta}$ ) to resolve the intermediate states in this three-body final state. For this purpose, we select events having  $-35 \text{ MeV} < \Delta E < 30 \text{ MeV}$ . This requirement corresponds to  $\pm 3.5\sigma$  ( $\pm 1.3\sigma$ ) of the narrower (wider) Gaussian. The  $B$  decay signal yield in this signal-enhanced region is  $403 \pm 35$  events.

The  $M_{J/\psi\eta}$  distribution for this subsample is shown in Fig. 2(a). We find a clear peak corresponding to the



TABLE I: Summary of the detection efficiency ( $\epsilon$ ), signal yield ( $N_{\text{sig}}$ ) and branching fraction ( $\mathcal{B}$ ) in  $-0.2 \text{ GeV}/c^2 < \Delta E < 0.2 \text{ GeV}/c^2$ , where the first and second errors are statistical and systematic.

Decay mode	$\epsilon(\%)$	$N_{\text{sig}}$	$\mathcal{B}$
$B^\pm \rightarrow J/\psi\eta K^\pm$	9.37	$428 \pm 37$	$(1.27 \pm 0.11 \pm 0.11) \times 10^{-4}$
$B^0 \rightarrow J/\psi\eta K_S^0$	7.23	$94 \pm 14$	$(5.22 \pm 0.78 \pm 0.49) \times 10^{-5}$

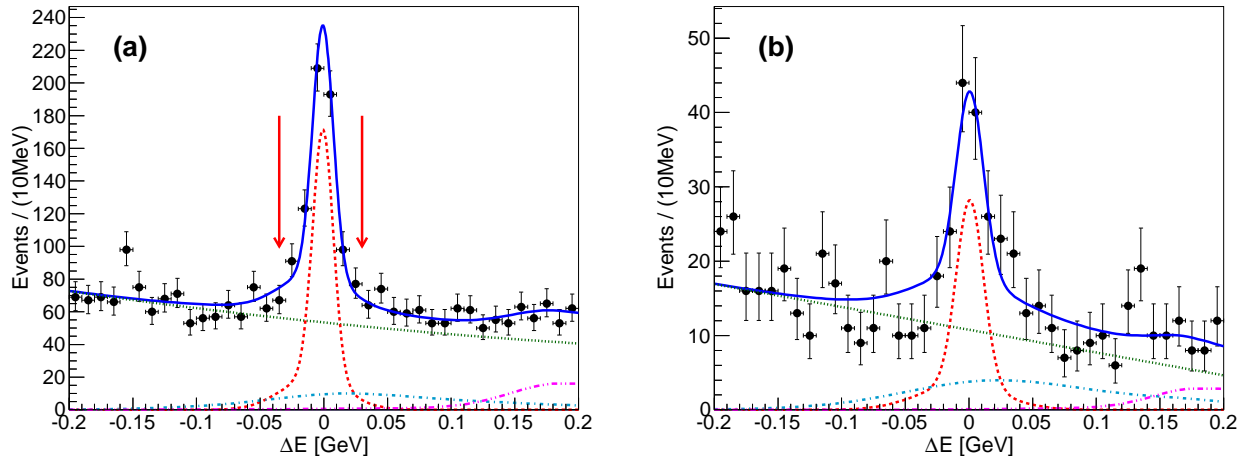


FIG. 1: (color online).  $\Delta E$  distribution of (a)  $B^\pm \rightarrow J/\psi\eta K^\pm$  and (b)  $B^0 \rightarrow J/\psi\eta K_S^0$  candidates in  $M_{bc} > 5.27 \text{ GeV}/c^2$ . Signal-enhanced region for  $B^\pm \rightarrow J/\psi\eta K^\pm$  is shown by the red arrows in (a). Data are shown by points with error bars. The red dashed line is signal, the cyan dot-dashed line is  $B \rightarrow \psi'(\not\rightarrow J/\psi\eta)K$  background, the magenta dot-dot-dashed line is  $B \rightarrow \chi_{c1}K$  background and the green dotted line is other backgrounds.

$\psi' \rightarrow J/\psi\eta$  decay at  $3686 \text{ MeV}/c^2$  with a yield of  $46 \pm 8$  events by performing an UML fit to the  $M_{J/\psi\eta}$  distribution in the range from the kinematical threshold to  $3770 \text{ MeV}/c^2$ . We parametrize the  $\psi'$  signal and remaining contributions by the sum of two Gaussians and a threshold function, respectively, as shown in Fig. 2(b). The  $\psi'$  shape is fixed to that found by a fit to the MC distribution, which is calibrated by the difference in resolution between data and simulation. The  $M_{J/\psi\eta}$  calibration factor is taken from the  $\Delta E$  distribution, since both resolutions are dominated by that of the  $\eta$  (reconstructed from photons rather than charged tracks). The threshold function is taken as  $a(M_{J/\psi\eta} - m_0)^{1/2} + b(M_{J/\psi\eta} - m_0)^{3/2} + c(M_{J/\psi\eta} - m_0)^{5/2}$ , where  $m_0 = 3.644 \text{ GeV}/c^2$  and the shape determined by  $a$ ,  $b$  and  $c$  is fixed to MC simulation; its normalization is floated in the fit. We obtain  $\mathcal{B}(B^\pm \rightarrow \psi' K^\pm)\mathcal{B}(\psi' \rightarrow J/\psi\eta) = (0.15 \pm 0.03(\text{stat.}) \pm 0.01(\text{syst.})) \times 10^{-4}$ , which is in agreement with the PDG value [10]. The rest of the  $B$  decay signal does not show any peaking structure and is consistent with three-body phase space.

The efficiency that is used to obtain the total branching fraction is determined by weighting the  $B^\pm \rightarrow \psi' K^\pm$  and the three-body phase components according to the observed  $M_{J/\psi\eta}$  spectrum. After subtracting the yield of  $46 \pm 8$  events for  $B^\pm \rightarrow \psi' K^\pm$  followed by  $\psi' \rightarrow J/\psi\eta$  (as described earlier), the remaining  $B$  decay signal yield is  $357 \pm 38$  events and is used to extract the branching fraction in Table II.

TABLE II: Summary of the detection efficiency ( $\epsilon$ ), signal yield ( $N_{\text{sig}}$ ) and branching fraction ( $\mathcal{B}$ ), where the first and second errors are statistical and systematic, respectively. For  $B^\pm \rightarrow \psi' K^\pm$ , followed by  $\psi' \rightarrow J/\psi\eta$ ,  $\mathcal{B}$  denotes the products of the branching fractions,  $\mathcal{B}(B^\pm \rightarrow \psi' K^\pm)\mathcal{B}(\psi' \rightarrow J/\psi\eta)$ . For the  $B^\pm$  decays, all relevant numbers are defined in the signal enhanced region,  $-35 \text{ MeV} < \Delta E < 30 \text{ MeV}$ .

Decay mode	$\epsilon(\%)$	$N_{\text{sig}}$	$\mathcal{B}$
$B^\pm \rightarrow J/\psi\eta K^\pm$ (Total)	8.82	$403 \pm 35$	$(1.27 \pm 0.11 \pm 0.11) \times 10^{-4}$
$B^\pm \rightarrow \psi' K^\pm, \psi' \rightarrow J/\psi\eta$	8.42	$46 \pm 8$	$(0.15 \pm 0.03 \pm 0.01) \times 10^{-4}$
$B^\pm \rightarrow J/\psi\eta K^\pm$ (excl. $\psi' K^\pm$ )	8.88	$357 \pm 38$	$(1.12 \pm 0.11 \pm 0.10) \times 10^{-4}$

The major source of systematic uncertainty in the branching fraction measurements is from the PDF uncertainty. It is estimated by varying all fixed parameters by  $\pm 1\sigma$  and summing all the variations in quadrature; it amounts

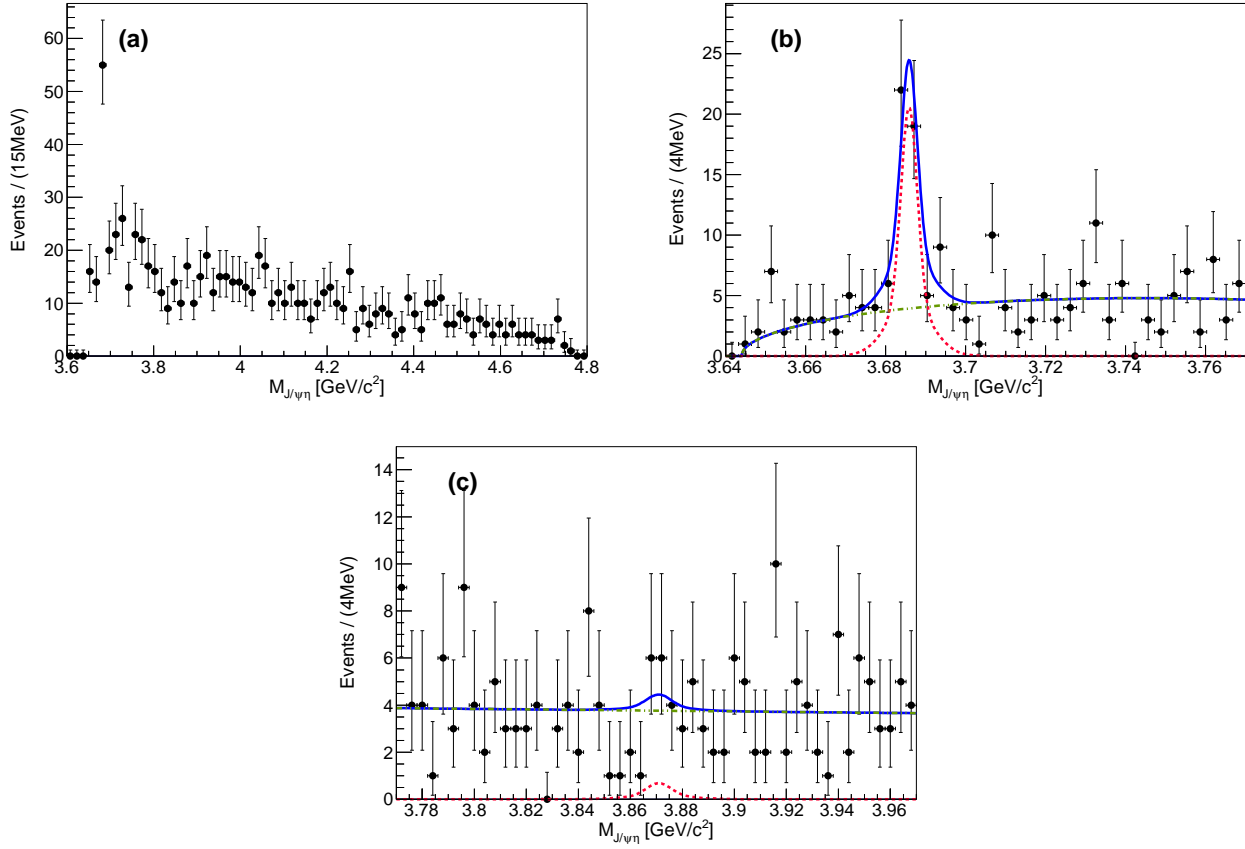


FIG. 2: (color online). The  $J/\psi\eta$  invariant mass ( $M_{J/\psi\eta}$ ) distribution of  $B^\pm \rightarrow J/\psi\eta K^\pm$  candidates for: (a) the entire mass distribution, (b) the region around the  $\psi'$  and (c) the  $X(3872)$  region. Data is shown by points with error bars; overall fit is shown by blue solid line. For (b) and (c), the red dashed line is for signal ( $\psi'$  and  $X(3872)$  in (b) and (c), respectively) and the green two dotted-dashed line is for the remainder.

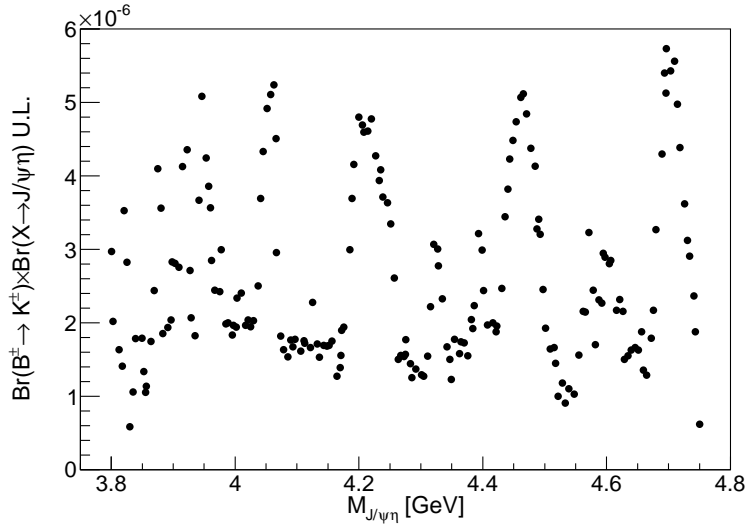


FIG. 3: 90% C.L. upper limit of the  $\mathcal{B}(B^\pm \rightarrow XK^\pm)\mathcal{B}(X \rightarrow J/\psi\eta)$  for a narrow resonance  $X$  as a function of the mass, with a  $5 \text{ MeV}/c^2$  interval.

to 7.3% for  $B^\pm \rightarrow J/\psi\eta K^\pm$  and 8.4% for  $B^0 \rightarrow J/\psi\eta K_S^0$ . The uncertainty of the tracking efficiency is estimated to be 0.35% per track. Small differences in the lepton and kaon identification efficiency between the data and MC simulation are included in the detection efficiency estimation and the relevant uncertainty is assigned as a systematic error. The uncertainty of electron identification is studied using the  $J/\psi \rightarrow e^+e^-$  sample and estimated to be 0.9% per  $e^+e^-$  pair. A similar approach for muon identification results in a systematic error of 3.9% per  $\mu^+\mu^-$  pair. A kaon identification uncertainty is determined to be 1.4% from the study using the  $D^{*+} \rightarrow D^0(\rightarrow K^-\pi^+)\pi^+$  sample. The uncertainty on the  $\eta \rightarrow \gamma\gamma$  efficiency is estimated to be 3.0% [37]. The  $K_S^0$  efficiency contributes a 0.7% error in the  $B^0 \rightarrow J/\psi\eta K_S^0$  mode. The uncertainties due to signal MC simulation statistics (0.5%) and the secondary branching fractions (0.7%) have only a small effect. The uncertainty of  $N_{B\bar{B}}$  is 1.4%. Table III summarizes the systematic uncertainties. The overall systematic error is obtained by adding all the contributions in quadrature; it is 8.6% for  $B^\pm \rightarrow J/\psi\eta K^\pm$  and 9.4% for  $B^0 \rightarrow J/\psi\eta K_S^0$ .

TABLE III: Contributions to the systematic uncertainty of the branching fraction. The value of PDF shape in parenthesis is for the  $B^\pm \rightarrow \psi' K^\pm$  decay followed by  $\psi' \rightarrow J/\psi\eta$ .

Source	Contribution (%)	
	$B^\pm \rightarrow J/\psi\eta K^\pm$	$B^0 \rightarrow J/\psi\eta K_S^0$
PDF shape ( $B^\pm \rightarrow \psi' K^\pm, \psi' \rightarrow J/\psi\eta$ )	7.3 (5.8)	8.4
Tracking efficiency	1.05	0.7
Lepton identification	2.4	2.4
Charged kaon identification	1.4	-
$\eta \rightarrow \gamma\gamma$ efficiency	3.0	3.0
$K_S^0 \rightarrow \pi^+\pi^-$ efficiency	-	0.7
Signal MC simulation stat.	0.5	0.5
Secondary $\mathcal{B}$	0.7	0.7
$N_{B\bar{B}}$	1.4	1.4
Total (inc. $\psi' K^\pm$ )	8.6 (7.4)	9.4

In order to probe the contribution of the  $X^{C\text{-odd}}$  partner assuming that it has same mass and width as the  $X(3872)$ , a sum of two Gaussians for signal and a first-order polynomial for background is used. For signal, all the parameters are fixed after applying the same MC-data shape-parameter calibrations used in the  $\psi'$  case. The  $X(3872)$  region is shown in Fig. 2(c). The fit result for the  $X^{C\text{-odd}}$  yield is found to be  $2.3 \pm 5.2$  events and we determine a 90% confidence level (C.L.) upper limit (U.L.) on the product of the branching fractions,  $\mathcal{B}(B^\pm \rightarrow X^{C\text{-odd}} K^\pm) \mathcal{B}(X^{C\text{-odd}} \rightarrow J/\psi\eta) < 3.8 \times 10^{-6}$ , using a frequentist approach. For a given signal yield, a large number of MC simulation sets, including signal and background components, are generated according to their PDFs, and a fit is performed to each set. The C.L. is determined from the fraction of sets that give a yield larger than the one observed in data. The input signal yield is varied until we obtain 90% C.L.; this input yield is the U.L. for the observed signal yield. To take into account the systematic uncertainty, the input signal yield for the simulated sets follows a Gaussian distribution whose width corresponds to the systematic uncertainty. This ensures that the yield fluctuations within the simulated sets exceeds those due solely to Poisson statistics. We divide the 3.8 to 4.8 GeV/ $c^2$  region into five 200 MeV/ $c^2$ -wide interval and use the PDF and efficiency estimated at 4070, 4270, 4470 and 4670 MeV/ $c^2$ . For the  $\psi(4040)$  and  $\psi(4160)$  cases, we describe the resonance by a Breit-Wigner function with the mass and width fixed to the values reported in Ref.[10]. Table IV summarizes the U.L. for the  $X^{C\text{-odd}}$  and  $\psi(4040, 4160)$ . As shown in Fig. 3, we also provide the U.L. at 90% C.L. of narrow resonances over a range from 3.8 to 4.8 GeV/ $c^2$ , with 5 MeV/ $c^2$  steps, using the same procedure as for the  $X^{C\text{-odd}}$  U.L. estimation.

TABLE IV: The U.L. for the product of the branching fractions  $\mathcal{B}(B^\pm \rightarrow X(\rightarrow J/\psi\eta)K^\pm) \equiv \mathcal{B}(B^\pm \rightarrow XK^\pm) \mathcal{B}(X \rightarrow J/\psi\eta)$  at 3872 and the  $\psi$  states recently found to decay into  $J/\psi\eta$ . Note that  $\epsilon$  is the corrected detection efficiency and the signal yield  $N_{\text{sig}}$  is given as an U.L. at 90% confidence level.

$M_X$ or $\psi$	$\epsilon$ (%)	$N_{\text{sig}}$	$\mathcal{B}(B^\pm \rightarrow X(\rightarrow J/\psi\eta)K^\pm)$
3872	8.1	$< 10.6$	$< 3.8 \times 10^{-6}$
$\psi(4040)$	9.2	$< 51.4$	$< 1.55 \times 10^{-5}$
$\psi(4160)$	9.2	$< 24.3$	$< 0.74 \times 10^{-5}$

In summary, we observe the  $B^\pm \rightarrow J/\psi\eta K^\pm$  and  $B^0 \rightarrow J/\psi\eta K_S^0$  decay modes and present the most precise measurements to date of the branching fractions,  $\mathcal{B}(B^\pm \rightarrow J/\psi\eta K^\pm) = (1.27 \pm 0.11(\text{stat.}) \pm 0.11(\text{syst.})) \times 10^{-4}$  and  $\mathcal{B}(B^0 \rightarrow J/\psi\eta K_S^0) = (5.22 \pm 0.78(\text{stat.}) \pm 0.49(\text{syst.})) \times 10^{-5}$ . For the  $B^\pm \rightarrow J/\psi\eta K^\pm$  signal, the  $M_{J/\psi\eta}$  distribution

is used to resolve each possible contribution to search for a resonance in the  $J/\psi\eta$  final state. Except for the known  $\psi' \rightarrow J/\psi\eta$  decay, the  $M_{J/\psi\eta}$  spectrum is found to be featureless and follows a non-resonant distribution. Because no signal is seen, we obtain an U.L. on the product of the branching fractions,  $\mathcal{B}(B^\pm \rightarrow X^{C\text{-odd}}K^\pm)\mathcal{B}(X^{C\text{-odd}} \rightarrow J/\psi\eta) < 3.8 \times 10^{-6}$  at 90% C.L.; this is less than one half of the corresponding value in  $X(3872) \rightarrow J/\psi\pi^+\pi^-$  [10]. While  $\psi(4040)$  and  $\psi(4160)$  decays into  $J/\psi\eta$  are observed in the initial state radiation process [23], production of those charmonia and their decays to the  $J/\psi\eta$  final state in  $B$  decays are found to be insignificant. The obtained U.L.s exclude a large branching fraction,  $\mathcal{O}(10^{-3})$ , for  $B^\pm \rightarrow \psi(4040)K^\pm$  and  $B^\pm \rightarrow \psi(4160)K^\pm$ . Nevertheless, values comparable to  $B^\pm \rightarrow \psi'K^\pm$  or  $B^\pm \rightarrow \psi(3770)K^\pm$ ,  $\mathcal{O}(10^{-4})$ , are still possible. Our results show that either the production of the  $C$ -odd partner of the  $X(3872)$  resonance in two-body  $B$  decay and/or its decay into  $J/\psi\eta$  is suppressed.

We thank the KEKB group for excellent operation of the accelerator; the KEK cryogenics group for efficient solenoid operations; and the KEK computer group, the NII, and PNNL/EMSL for valuable computing and SINET4 network support. We acknowledge support from MEXT, JSPS and Nagoya's TLPRC (Japan); ARC and DIISR (Australia); FWF (Austria); NSFC (China); MSMT (Czechia); CZF, DFG, and VS (Germany); DST (India); INFN (Italy); MEST, NRF, GSDC of KISTI, and WCU (Korea); MNiSW and NCN (Poland); MES and RFAAE (Russia); ARRS (Slovenia); IKERBASQUE and UPV/EHU (Spain); SNSF (Switzerland); NSC and MOE (Taiwan); and DOE and NSF (USA). This work is partly supported by Grant-in-Aid from MEXT for Scientific Research on Innovative Areas ("Elucidation of New hadrons with a Variety of Flavors").

- 
- [1] S.-K. Choi *et al.* (Belle Collaboration), Phys. Rev. Lett. **91**, 262001 (2003).  
[2] N. Brambilla *et al.*, Eur. Phys. J. C **71**, 1534 (2011).  
[3] T. Aushev *et al.* (Belle Collaboration), Phys. Rev. D **81**, 031103 (2010); B. Aubert *et al.* (BaBar Collaboration), Phys. Rev. D **77**, 011102 (2008).  
[4] P. del Amo Sanchez *et al.* (BaBar Collaboration), Phys. Rev. D **82**, 011101 (2010).  
[5] B. Aubert *et al.* (BaBar Collaboration), Phys. Rev. Lett. **102**, 132001 (2009).  
[6] V. Bhardwaj *et al.* (Belle Collaboration), Phys. Rev. Lett. **107**, 091803 (2011).  
[7] A. Abulencia *et al.* (CDF collaboration), Phys. Rev. Lett. **98**, 132002 (2007).  
[8] S.-K. Choi *et al.* (Belle Collaboration), Phys. Rev. D **84**, 052004 (2011).  
[9] R. Aaij *et al.* (LHCb Collaboration), Phys. Rev. Lett. **110**, 222001 (2013).  
[10] J. Beringer *et al.* (Particle Data Group), Phys. Rev. D **86**, 010001 (2012) and 2013 particle update for the 2014 edition.  
[11] E.S. Swanson, Phys. Lett. B **598**, 197 (2004); E.S. Swanson, Phys. Rep. **429**, 243 (2006).  
[12] L. Maiani, F. Piccinini, A.D. Polosa and V. Riquer, Phys. Rev. D **71**, 014028 (2005).  
[13] B.A. Li, Phys. Lett. B **605**, 306 (2005).  
[14] M. Suzuki, Phys. Rev. D **72**, 114013 (2005).  
[15] K. Terasaki, Prog. Theor. Phys. **127**, 577 (2012).  
[16] J. Nieves and M. Pavón Valderrama, Phys. Rev. D **86**, 056004 (2012).  
[17] B. Aubert *et al.* (BaBar Collaboration), Phys. Rev. D **71**, 031501 (2005).  
[18] V. Bhardwaj *et al.* (Belle Collaboration), Phys. Rev. Lett. **111**, 032001 (2013).  
[19] D. Ebert, R.N. Faustov and V.O. Galkin, Phys. Rev. D **67**, 014027 (2003).  
[20] P. Ko, J. Lee and H.S. Song, Phys. Lett. B **395**, 107 (1997).  
[21] C.-F. Qiao, F. Yuan and K.-T. Chao, Phys. Rev. D **55**, 4001 (1997).  
[22] M. Ablikim *et al.* (BESIII Collaboration), Phys. Rev. D **86**, 071101 (2012).  
[23] X.L. Wang *et al.* (Belle Collaboration), Phys. Rev. D **87**, 051101 (2013).  
[24] M. Beneke, G. A. Schuler, and S. Wolf, Phys. Rev. D **62**, 034004 (2000).  
[25] R. Balest *et al.* (CLEO Collaboration), Phys. Rev. D **52**, 2661 (1995); S. Anderson *et al.* Phys. Rev. Lett. **89**, 282001 (2002).  
[26] B. Aubert *et al.* (BABAR Collaboration), Phys. Rev. D **67**, 032002 (2003).  
[27] C.-K. Chua and W.-S. Hou, Phys. Rev. D **68**, 054012 (2003).  
[28] T. J. Burns, F. Piccinini, A. D. Polosa, V. Prospero, and C. Sabelli, Phys. Rev. D **83**, 114029 (2011).  
[29] B. Aubert *et al.* (BaBar Collaboration), Phys. Rev. Lett. **93**, 041801 (2004).  
[30] Inclusion of charge-conjugate modes is implied.  
[31] S. Kurokawa and E. Kikutani, Nucl. Instrum. Methods Phys. Res., Sect. A **499**, 1 (2003), and other papers included in this volume; T. Abe *et al.*, Prog. Theor. Exp. Phys. (2013) 03A001 and following articles up to 03A011.  
[32] A. Abashian *et al.* (Belle Collaboration), Nucl. Instrum. Methods Phys. Res., Sect. A **479**, 117 (2002); see also the detector section in J. Brodzicka *et al.*, Prog. Theor. Exp. Phys. (2012) 04D001.  
[33] Z. Natkaniec *et al.* (Belle SVD2 Group), Nucl. Instrum. Methods Phys. Res., Sect. A **560**, 1 (2006).  
[34] A. Abashian *et al.* (Belle Collaboration), Nucl. Instrum. Methods Phys. Res., Sect. A **491**, 69 (2002).  
[35] K.-F. Chen *et al.* (Belle Collaboration), Phys. Rev. D **72**, 012004 (2005).



- [36] G.C. Fox and S. Wolfram, Phys. Rev. Lett. **41**, 1581 (1978).
- [37] M.-C. Chang *et al.* (Belle Collaboration), Phys. Rev. D **85**, 091102(R) (2012).